Cell, Vol. 112, 779–791, March 21, 2003, Copyright ©2003 by Cell Press

Pirh2, a p53-Induced Ubiquitin-Protein Ligase, Promotes p53 Degradation

Roger P. Leng,[1] Yunping Lin,[1] Weili Ma,[1] Hong Wu,[2] Benedicte Lemmers,[1,3] Stephen Chung,[1] John M. Parant,[4] Guillermina Lozano,[4] Razqallah Hakem,[1,3] and Samuel Benchimol[1,*]

[1]Ontario Cancer Institute and Department of Medical Biophysics
University of Toronto
610 University Avenue
Toronto
Ontario
Canada M5G 2M9

[2]The Hospital for Sick Children
555 University Avenue
Toronto
Ontario
Canada M5G 1X8

[3]Advanced Medical Discovery Institute
University Health Network
620 University Avenue
Toronto
Ontario
Canada M5G 2C1

[4]Department of Molecular Genetics
The University of Texas
M.D. Anderson Cancer Center
Houston, Texas 77030

Summary

The p53 tumor suppressor exerts anti-proliferative effects in response to various types of stress including DNA damage and abnormal proliferative signals. Tight regulation of p53 is essential for maintaining normal cell growth and this occurs primarily through post-translational modifications of p53. Here, we describe Pirh2, a gene regulated by p53 that encodes a RING-H2 domain-containing protein with intrinsic ubiquitin-protein ligase activity. Pirh2 physically interacts with p53 and promotes ubiquitination of p53 independently of Mdm2. Expression of Pirh2 decreases the level of p53 protein and abrogation of endogenous Pirh2 expression increases the level of p53. Furthermore, Pirh2 represses p53 functions including p53-dependent transactivation and growth inhibition. We propose that Pirh2 is involved in the negative regulation of p53 function through physical interaction and ubiquitin-mediated proteolysis. Hence, Pirh2, like Mdm2, participates in an autoregulatory feedback loop that controls p53 function.

Introduction

The ability of p53 protein to inhibit cell cycling or promote apoptosis is closely associated with its tumor suppressor function. In this way, cells that are growing inappropriately or that have been subjected to deleterious stress or DNA damage are given time to repair the damage or are eliminated from the population (Levine, 1997; Vogelstein et al., 2000). p53 protein is positively regulated through a succession of posttranslational modifications including phosphorylation and acetylation (Appella and Anderson, 2001). In its inactive form, p53 is bound to Mdm2 protein. Binding to Mdm2 inhibits the transcriptional activity of p53 (Momand et al., 1992; Oliner et al., 1993) and promotes the degradation of p53 by the 26S proteasome (Haupt et al., 1997; Kubbutat et al., 1997; Honda et al., 1997). Mdm2 is an E3 ubiquitin ligase for p53 (Honda et al., 1997; Honda and Yasuda, 2000; Fang et al., 2000) and is itself the product of a p53-inducible gene. This dependency creates an autoregulatory feedback loop in which both the activity of p53 protein and the expression of Mdm2 are regulated (Barak et al., 1993; Wu et al., 1993). Stress-induced phosphorylation of two critical residues on p53, Ser15 and Ser20, results in Mdm2 dissociation and stabilization of p53 (Vousden, 2002). Subsequent phosphorylation and acetylation leads to activation of the sequence-specific DNA binding and transcriptional activities of p53 (Appella and Anderson, 2001; Prives and Manley, 2001). The physiological significance of the p53:Mdm2 interaction was dramatically illustrated by the finding that deletion of *Mdm2* in the mouse resulted in embryonic lethality, and that simultaneous loss of *p53* completely rescued this phenotype (Montes de Oca Luna et al., 1995; Jones et al., 1995). JNK has also been shown to bind to the central domain of p53 (residues 97–155) in nonstressed cells and to promote ubiquitination and degradation of p53 independently of Mdm2 (Adler et al., 1997; Fuchs et al., 1998). Experiments performed in JNK-depleted, Mdm2 null extracts in which p53 ubiquitination was reduced but not abolished, suggested the existence of other molecules capable of targeting p53 for ubiquitination (Fuchs et al., 1998).

Here, we describe a gene regulated by p53 that encodes a predicted protein of 261 amino acids, which we have named Pirh2. We present evidence that Pirh2 can directly bind p53 protein both in vitro and in vivo, and that it can repress p53-dependent transactivation and growth suppression. Pirh2 contains a RING-H2 domain and has intrinsic E3 ubiquitin ligase activity. We show that Pirh2 regulates the steady-state level of p53 protein and that it promotes ubiquitination of p53 independently of Mdm2. Hence, Pirh2, like Mdm2, participates in an autoregulatory feedback loop that serves to control p53 function.

Results

Identification of *Pirh2*, a p53-Inducible Gene that Encodes a RING-H2 Protein

To identify p53-target genes, we used the method of differential display and a mouse cell line containing a temperature-sensitive p53 allele, DP16.1/p53ts (Johnson et al., 1993). We detected a 1.7 kb transcript that was reproducibly more abundant in DP16.1/p53ts cells

*Correspondence: benchimo@uhnres.utoronto.ca

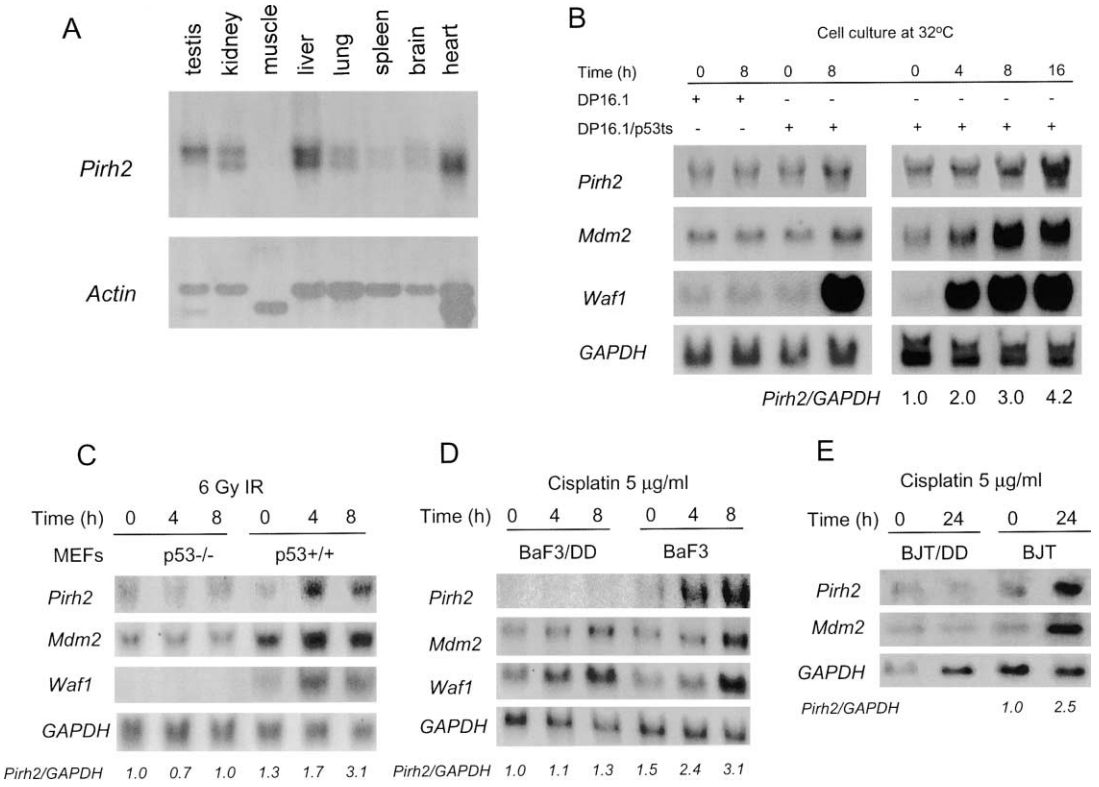

Figure 1. p53 Activates *Pirh2* Expression

(A) Northern blot in which polyA$^+$ RNA from multiple mouse tissues (Clontech) was hybridized with a mouse *Pirh2* cDNA probe. Two *Pirh2* transcripts of approximately 1.6- and 1.7 kb were detected. *Actin* expression was examined as a loading control.

(B) RNA was isolated from parental DP16.1 cells and DP16.1/p53ts cells after incubation at 32°C for the times indicated. RNA (10 μg) was run in each lane and hybridized to *Pirh2*, *Mdm2*, *p21^{WAF1}*, and *GAPDH* cDNA probes. RNA was visualized by autoradiography. The relative abundance of *Pirh2* mRNA was determined by phosphorimage analysis after normalizing to the level of *GAPDH* mRNA in each sample.

(C) Northern blot analysis of RNA isolated from wild-type (p53$^{+/+}$) and p53$^{-/-}$ early passage MEFs before and after γ-irradiation with a dose of 6 Gy at the times indicated. The blot was hybridized with the indicated cDNA probes and analyzed as in (B).

(D–E) Northern blot analysis of RNA isolated from mouse BaF3 and BaF3/DD cells, and from human BJT and BJT/DD cells treated with cisplatin for the times indicated. The blot was hybridized with the indicated cDNA probes and analyzed as in (B).

cultured at 32°C compared with parental DP16.1 cells grown at 32°C and DP16.1/p53ts cells grown at 37°C. Using the differential display fragment representing this transcript and 5′RACE, and a combination of database searching and RT-PCR analyses, we obtained a cDNA clone with an insert of 1226 bp. This sequence includes an open reading frame that encodes a 261 amino acid protein with a predicted molecular mass of 30 kDa (see Supplemental Figure S1 available at http://www.cell.com/cgi/content/full/112/6/779/DC1). The predicted protein contains a cysteine-rich RING motif defined by the consensus sequence **CXXCX**(9,39)**CX**(1,3)**HX**(2,3)**C/HXXCX**(4,48)**CXXC** with eight cysteines and histidines that coordinate two zinc ions (Borden, 2000). We have named this protein Pirh2 (for p53-induced protein with a RING-H2 domain).

Northern blot analysis of RNA from various adult mouse tissues identified two *Pirh2* mRNA transcripts with approximate lengths of 1.7 kb and 1.6 kb (Figure 1A). *Pirh2* mRNA expression was highest in the liver; relatively high levels were expressed in testis and heart, and lower levels were expressed in muscle and spleen.

To confirm that *Pirh2* is a p53-regulated gene, we studied the kinetics of *Pirh2* induction in DP16.1/p53ts cells in response to p53 activation at 32°C by Northern blot analysis (Figure 1B). *Pirh2* mRNA levels increased within 4 hr of p53 activation and reached their highest levels at 16 hr (4.2-fold). The amount of *Pirh2* mRNA was unchanged in DP16.1 cells at 32°C, indicating that *Pirh2* mRNA induction in DP16.1/p53ts cells is dependent on p53 and not simply the result of a change in temperature. In comparison, *Mdm2* and *p21^{WAF1}* induction in DP16.1/p53ts cells was strongest at 8 hr (2.6-fold and 9.3-fold, respectively).

RNA samples from various cell lines were examined by Northern blotting to investigate the relationship between p53 and *Pirh2* expression. *Pirh2* mRNA was induced in response to γ-irradiation in wild-type MEFs (2.4-fold) but not in *p53$^{-/-}$* MEFs (Figure 1C). We also observed induction of *Pirh2* mRNA in response to cisplatin treatment in the wild-type p53-expressing, murine pro B cell line, BaF3 (2.1-fold), but not in BaF3/DD cells, an isogenic derivative expressing the C-terminal fragment of p53 (Figure 1D). This fragment has been shown to act as a potent trans-dominant repressor of wild-type p53 through its ability to prevent the formation of functional p53 tetramers (Shaulian et al., 1992). In addition, we saw an increase in *Pirh2* expression in cisplatin-treated

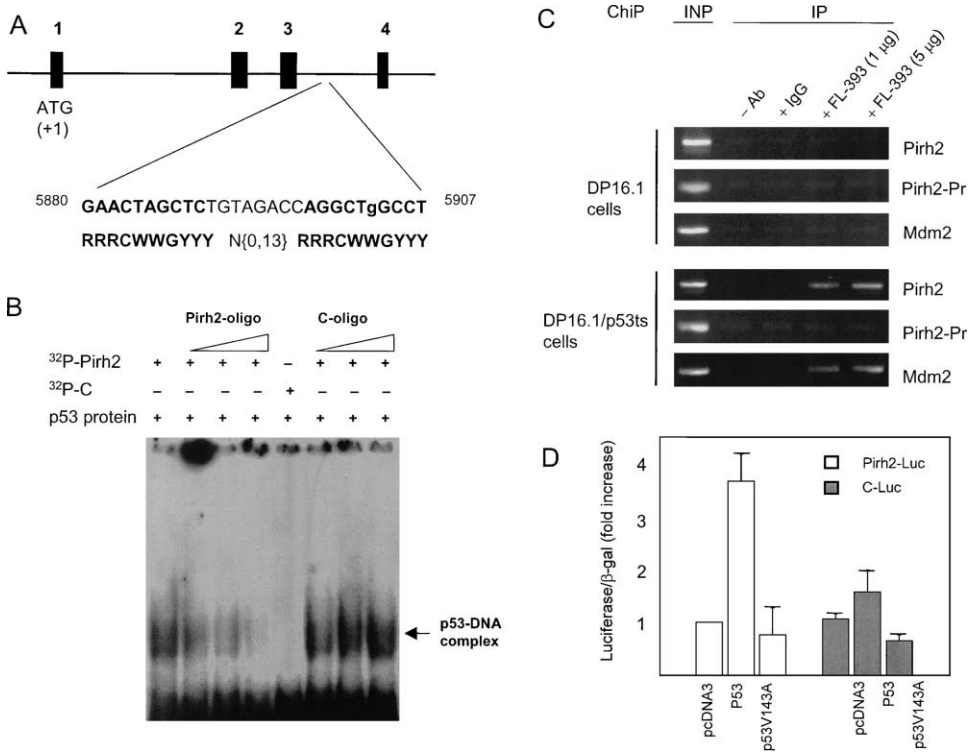

Figure 2. The p53-Consensus Binding Sequence in *Pirh2* is Responsive to p53

(A) The potential p53 binding site in intron 3 of the mouse *Pirh2* gene is indicated above the p53 consensus binding site (El-Deiry et al., 1992), with R denoting purine, Y denoting pyrimidine, and W denoting A or T. The numbering is relative to the first nucleotide of the proposed ATG initiator methionine. The four exons shown cover only the first 135 amino acids of the Pirh2 open reading frame. The potential p53 binding site in *Pirh2* matches the consensus at 19 out of 20 nucleotides.

(B) Electrophoretic mobility shift assays were performed with purified truncated p53 (residues 82–360). Binding reactions were performed with a ^{32}P-labeled double-stranded oligonucleotide containing the p53 consensus binding sequence in *Pirh2* or with an unrelated C oligonucleotide having the same nucleotide composition. Unlabeled cold competitor (double-stranded *Pirh2* or unrelated C oligonucleotide) was added at 10-fold, 50-fold, and 100-fold molar excess over the labeled *Pirh2* oligonucleotide.

(C) Chromatin immunoprecipitation assay of p53 DNA binding activity in p53-expressing DP16.1/p53ts cells and parental p53 null DP16.1 cells. DP16.1/p53ts cells were cultured at 32°C and harvested 8 hr later. A rabbit polyclonal antibody to p53 (FL-393) or control rabbit IgG was used. PCR analysis (using primers to intron 3 of *Pirh2* or *Pirh2* promoter or intron 1 of *Mdm2*) is shown using input DNA (1/20 of ChIP) or DNA after ChIP. Amplification products ranged in length from 200 bp to 240 bp.

(D) Histogram representing the ability of wild-type p53 or the p53V143A mutant to transactivate a luciferase reporter bearing the p53 binding sequence from *Pirh2* (Pirh2-Luc) or an unrelated control sequence (C-Luc). A β-galactosidase reporter construct was included in all the transfection mixes and used for normalization. Error bars indicate SEM (n = 8).

human BJT fibroblasts (2.5-fold) but not in the isogenic derivative, BJT/DD, expressing the dominant-negative C-terminal fragment of p53 (Figure 1E). We also observed induction of *Pirh2* mRNA in response to γ-irradiation and UV-irradiation in mouse ES cells (data not shown). We did not detect any increase in the level of *Pirh2* mRNA after γ-irradiation in two wild-type p53 expressing cell lines that we tested (MCF-7 and OCI/AML-4) (data not shown). Moreover, we did not detect any increase in the level of *Pirh2* in UV-irradiated MEFs or in UV- or γ-irradiated BJT cells. Hence, the induction of *Pirh2* mRNA by p53 appears to be dependent on cell type and the DNA damaging agent used to activate p53.

Intron 3 of *Pirh2* Contains a p53 Binding Site

Isolation and examination of mouse genomic sequences covering the first four exons of *Pirh2*, including 8.6 kbp upstream of the first exon, revealed the presence of a putative p53 binding site within the third intron of *Pirh2* (Figure 2A). This site matched the consensus p53 binding site at 19 out of 20 base pairs and contained an 8 bp spacer between the two half-sites. Electrophoretic mobility shift experiments indicated that p53 bound the *Pirh2* element but not an unrelated control sequence (Figure 2B). We also tested the binding of p53 to the *Pirh2* intron 3 site using chromatin immunoprecipitation (ChIP). DP16.1/p53ts cells were grown at 32°C for 8 hr and subjected to ChIP analysis by immunoprecipitation with control IgG or p53-specific polyclonal antibody (FL-393), followed by PCR analysis of the of the *Pirh2* intron 3 region surrounding the p53 response element. Amplification of the *Pirh2* promoter (*Pirh2*-Pr) and of a region containing a p53 binding site in the first intron of the *Mdm2* gene (Juven et al., 1993; Wu et al., 1993) served as negative and positive controls, respectively. The data presented in Figure 2C show that *Pirh2* intron 3 was bound by p53 in vivo.

To determine whether p53 activates transcription of a minimal promoter containing the p53 binding sequence present in intron 3 of *Pirh2*, a double-stranded oligonu-

cleotide containing one copy of this element was inserted into the luciferase reporter vector pGL3E1bTATA (designated Pirh2-Luc). Human Saos2 osteosarcoma cells, which harbor a homozygous deletion of the *p53* locus and do not produce p53 protein, were transfected with Pirh2-Luc along with plasmids expressing either wild-type p53 or mutant p53 (p53 V143A). Wild-type p53 enhanced luciferase expression from Pirh2-Luc moderately, 3.7-fold. p53 V143A had no activity in these assays (Figure 2D). In comparison, we found that luciferase expression from reporter plasmids containing the p53 binding site from $p21^{WAF1}$ or from *Mdm2* were stimulated 57-fold and 11-fold, respectively, by p53 (data not shown). Collectively, these data indicate that the DNA sequence within intron 3 of mouse *Pirh2* (between bases 5880 and 5907) constitutes a bona fide p53 binding site.

Physical Interaction of Pirh2 with p53

Polyclonal antibodies against bacterially expressed human and mouse Pirh2 proteins were produced in rabbits (see Supplemental Figure S2 available at http://www.cell.com/cgi/content/full/112/6/779/DC1). Using these antibodies for Western blotting, we detected an increase in the level of Pirh2 protein in DP16.1/p53ts cells but not parental DP16.1 cells when these cells were shifted to 32°C to activate p53 (Figure 3A). We also detected increased expression of Pirh2 protein in irradiated MEFs as well as in cisplatin-treated BaF3 and BJT cells (Figure 3B) consistent with the RNA data shown in Figure 1. In each of these experimental models, increased Pirh2 expression was dependent on p53.

Plasmids expressing Pirh2 and p53 were cotransfected into Saos2 cells. The transfected cells were labeled with [^{35}S]methionine/cysteine and protein extracts were subjected to immunoprecipitation with the Pirh2 antibody. Radiolabeled Pirh2 protein was detected in cells transfected with the Pirh2 cDNA plasmid and not in cells transfected with the empty pcDNA3 vector. Coimmunoprecipitation of a 53 kDa protein was seen only in cells cotransfected with Pirh2 and p53 expression plasmids (Figure 3C). To confirm that the 53 kDa protein was p53, we performed an IP/Western blotting experiment using extracts prepared from Saos2 cells that had been transiently transfected with plasmids expressing p53, Pirh2, and various Pirh2 mutants that disrupt the RING domain. Extracts were mixed with the Pirh2 antibody and the resulting immune complexes were collected and analyzed by immunoblotting with the p53-specific monoclonal antibody PAb1801 (Figure 3D, top image) or with antibodies to Pirh2 (Figure 3D, bottom image). p53 coimmunoprecipitated with Pirh2. Binding between these molecules appeared not to be dependent on the RING-H2 domain of Pirh2. Next, Saos2 cells were cotransfected with plasmids expressing His-tagged Pirh2 and p53, and the extracts were immunoprecipitated with a monoclonal antibody against His. p53 protein was detected in the anti-His immunoprecipitate confirming the in vivo interaction between p53 and Pirh2 (Figure 3D). Next, we performed an in vitro GST pull-down assay. Cell extracts were prepared from DP16.1 cells ectopically expressing mouse p53 and from Saos2 cells ectopically expressing human p53. p53 protein present in these extracts bound to immobilized GST-Pirh2 but not to GST alone (Figure 3E). Finally, we wished to determine if endogenous p53 and Pirh2 could interact under more physiological conditions in the absence of ectopic overexpression. An IP/Western blotting experiment was performed using extracts prepared from human BJT fibroblasts. We observed that p53 coimmunoprecipitated with Pirh2. In the reciprocal experiment using PAb1801 antibodies to immunoprecipitate p53, we observed that Pirh2 coimmunoprecipitated with p53 (Figure 3F). We conclude that p53 and Pirh2 physically interact in vivo.

Residues 120 to 137 of Pirh2 Are Required for Binding to p53

To identify the region of Pirh2 that interacts with p53, a series of Pirh2 deletion mutants was expressed in bacteria as GST-fusion proteins (Figure 4A, top image). These were employed in a GST-pull-down assay with ^{35}S-labeled in vitro translated p53 protein (Figure 4A, bottom image, left). All of the Pirh2 fragments, with the exception of an N-terminal fragment containing the first 60 amino acids, were capable of binding to p53. The data, summarized in Figure 4B, indicate that a region of Pirh2 encompassing residues 120 to 137 is required for binding p53. To confirm this finding, a GST-Pirh2 fusion protein lacking residues 120–137 was expressed and used in a GST pull-down assay. This deletion mutant was unable to bind p53 (Figure 4A, middle image). To investigate whether the binding between p53 and Pirh2 is direct or indirect, purified GST-Pirh2 was mixed with purified His-tagged p53. Protein complexes were collected with glutathione-agarose beads and the presence of bound p53 assessed by immunoblotting with anti-His antibody (Figure 4A, right image). p53 bound to full-length GST-Pirh2 but not to GST-Pirh2 Δ120–137 or to GST. We conclude that p53 binds directly to Pirh2.

The Central Region of p53 (Residues 82–292) Binds Pirh2

To identify the region of p53 required for the association with Pirh2, we performed pull-down assays with in vitro translated ^{35}S-labeled Pirh2 and a series of bacterially expressed p53 deletion mutants tagged with GST or His (Figure 4C, top image). The region of p53 extending from residues 82 to 292 exhibited binding to Pirh2, while neither a p53 fragment containing only the N-terminal portion, nor a p53 fragment containing only the C-terminal portion was capable of binding Pirh2 (Figure 4C, bottom).

Pirh2 Expression Reduces the Amount of Endogenous p53 Protein

We tested the ability of Pirh2 to regulate the level of endogenous wild-type p53 protein in MCF-7 cells. Transient overexpression of Pirh2 resulted in a reduction in the level of p53 (Figure 5A). In addition, we tested whether endogenous Pirh2 is critical in regulating the level of p53 protein in BJT cells. An antisense oligonucleotide directed against *Pirh2* effectively inhibited Pirh2 expression in BJT cells while a control-scrambled oligonucleotide had no effect (Figure 5B). Importantly the decrease in Pirh2 was accompanied by an increase in the level of endogenous p53 protein (Figure 5B). Next,

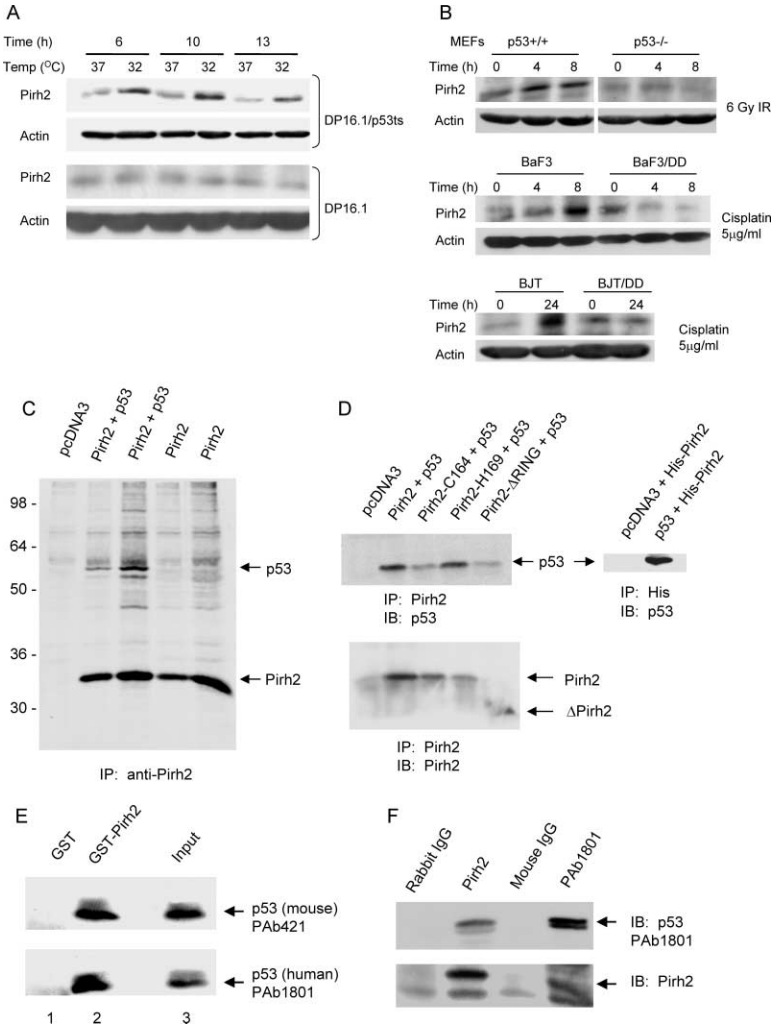

Figure 3. Interaction between p53 and Pirh2

(A) DP16.1/p53ts and DP16.1 cells were cultured at 37°C or at 32°C for the times indicated. Immunoblot showing Pirh2 protein accumulation in response to p53 activation. An antibody against β-actin was used as a loading control.

(B) Immunoblot showing Pirh2 protein levels in γ-irradiated MEFs ($p53^{+/+}$ and $p53^{-/-}$), cisplatin-treated BaF3 and BaF3/DD cells, and cisplatin-treated BJT and BJT/DD cells.

(C) p53 null Saos2 cells were transfected with the indicated expression plasmids in duplicate; 24 hr later, the cells were metabolically labeled with ^{35}S-methionine/cysteine for 2 hr and extracts were prepared. Pirh2 protein was immunoprecipitated, the immune complexes were collected with protein A Sepharose beads, resolved by SDS-PAGE, and visualized by autoradiography.

(D) Saos2 cells were transfected with p53 and Pirh2 expression plasmids as indicated. Equal amounts of cell extract were immunoprecipitated with the Pirh2 antibody (left) or with an antibody directed against His (right) and analyzed by immunoblotting following SDS-PAGE with antibodies directed against p53 (PAb1801) or against Pirh2.

(E) In vitro interaction of Pirh2 and p53 protein evaluated in GST pull-down assays. The ability of mouse p53 (top) or human p53 protein (bottom) present in cell extracts to be retained by GST (lane 1) or GST-Pirh2 fusion protein (lane 2) was analyzed by immunoblotting following SDS-PAGE. A total of 1 μg GST and 1 μg GST-Pirh2 were applied to glutathione beads. p53 was visualized by immunoblot analysis of the glutathione-agarose complexes using antibodies to mouse (PAb421) or human (PAb1801) p53. Input (50 μg of extract) represents 1/6 of that used for GST pull-down.

(F) Cell extracts were prepared using human BJT fibroblasts. Equal amounts of extract were immunoprecipitated with the indicated antibodies and analyzed by immunoblotting with antibodies to detect p53 (PAb1801) or Pirh2.

we generated a series of MCF-7 clones that stably express hPirh2, Mdm2, or various hPirh2 mutants: ΔRING (containing an internal deletion of the RING-H2 domain that removes residues 145 to 186), and C164A and H169A (in which the metal coordinating residues Cys164 and His169 within the RING-H2 domain are replaced with Ala). The immunoblot shown in Figure 5C indicates lower levels of endogenous p53 protein in clones expressing Pirh2 or Mdm2 in comparison with clones expressing Pirh2 RING mutants or with clones containing the empty vector. p53 mRNA levels were not affected by ectopic expression of Pirh2 (data not shown) indicating that p53 protein is the target of Pirh2. Together, these data indicate that Pirh2, like Mdm2, can regulate the steady-state level of p53 protein.

Pirh2 Has Ubiquitin-Protein Ligase Activity

To determine if Pirh2, like Mdm2, can mediate protein ubiquitination in vivo, vectors expressing Pirh2, Mdm2, and HA-tagged ubiquitin were transfected into Saos2 cells. Cell extracts were subjected to immunoblotting with antibodies to Pirh2, Mdm2, or HA. Mdm2 and Pirh2 were expressed in the transfected cells (Figure 6A) and caused a large increase in protein ubiquitination that was not seen in the absence of co-expressed HA-tagged ubiquitin (Figure 6A, compare lanes 7 and 8 with lanes 3 and 4).

To determine if Pirh2 can promote ubiquitination of p53 in vivo, p53 and HA-tagged ubiquitin were co-expressed in Saos2 cells together with Pirh2 or Mdm2. Ectopically expressed p53 appeared as a doublet in these experiments; the smaller species may be the result of degradation or internal initiation. Importantly the overall level of p53 was lower when p53 was co-expressed with Pirh2 or Mdm2 (Figure 6A, lanes 2, 6, 9, and 10; Figure 6B, lanes 3–5) consistent with our previous results. We observed a massive increase in the amount of protein ubiquitination when p53 was co-expressed with Mdm2 or with Pirh2 (Figure 6A, lanes 9 and 10). This level of ubiquitination was not seen with p53 alone

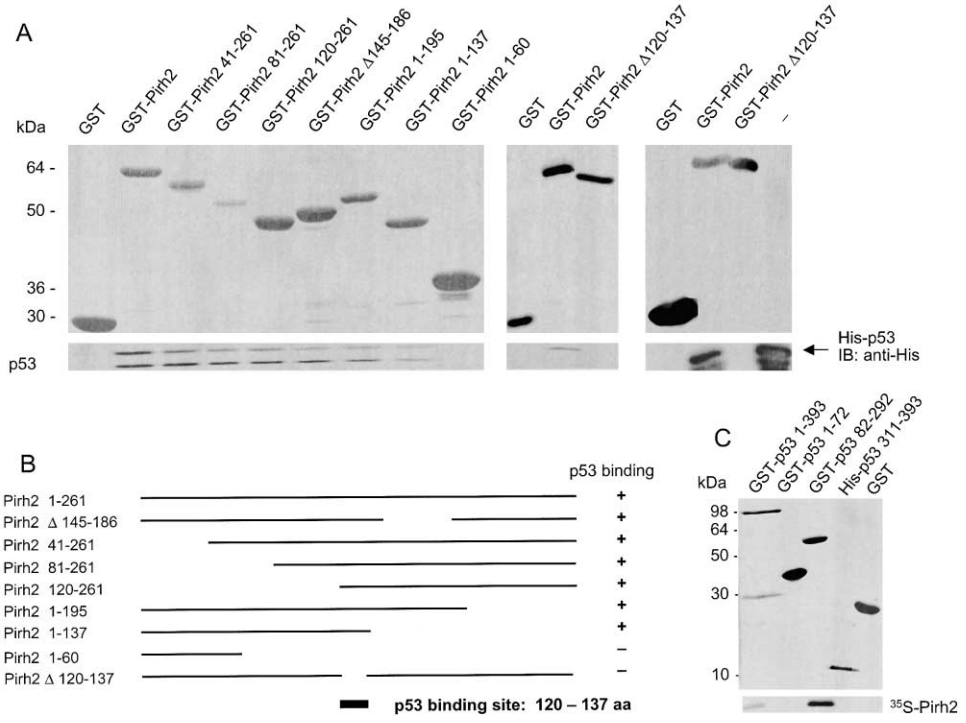

Figure 4. Mapping the Interaction Sites on Pirh2 and p53

(A) The region of Pirh2 involved in binding to p53 was analyzed in GST pull-down assays. GST-Pirh2 fusion proteins were affinity purified and analyzed by SDS-PAGE and Coomassie blue staining (top). The ability of the various truncated Pirh2 fusion proteins to bind to in vitro translated ^{35}S-labeled p53 protein (left image) or to unlabeled in vitro translated p53 protein (middle image) or to purified His-p53 fusion protein (right image) was analyzed by SDS-PAGE and autoradiography (left bottom image) or by immunoblotting with PAb1801 antibodies against p53 (middle bottom image) or by immunoblotting with antibodies against His (right bottom image), respectively. The right lane in the right image represents the input His-p53 protein used in the binding reaction.

(B) Schematic representation of Pirh2 truncations fused to GST. The binding site for p53, based on the data provided in (A), is indicated.

(C) The region of p53 involved in binding to Pirh2 was analyzed in pull-down assays. GST-p53 or His-p53 fusion proteins were affinity purified and analyzed by SDS-PAGE and Coomassie blue staining (top). The ability of the various p53 fusion proteins to bind to in vitro translated ^{35}S-labeled Pirh2 was analyzed by SDS-PAGE and autoradiography (bottom).

(Figure 6A, lane 6). In parallel experiments, p53 was immunoprecipitated with PAb1801 antibodies and analyzed by immunoblotting with HA antibodies to detect ubiquitinated p53 (Figure 6B, top image) or with Ab-7 to detect all the p53 (Figure 6B, bottom image). p53 (or proteins that coimmunoprecipitate with p53) appeared heavily ubiquitinated in the presence of Mdm2 and to a lesser extent in the presence of Pirh2 (Figure 6B, top image). The p53 immunoblot (Figure 6B, bottom image) revealed the presence of high molecular weight species of p53 generated in the presence of Mdm2 or Pirh2 that are consistent with ubiquitination. The distribution of p53-related species observed on the blot suggests that Pirh2 may be more proficient at polyubiquitination than Mdm2.

These experiments were performed in Mdm2-positve cells and, as a result, they raised the question of whether Pirh2 was promoting ubiquitination through Mdm2. To investigate the possible relationship between Pirh2 and Mdm2, we compared the ubiquitination promoting activity of ectopically expressed Pirh2 and Mdm2 in p53$^{-/-}$ Mdm2$^{-/-}$ double-null MEFs. As indicated in Figure 6C, Pirh2 promoted protein ubiquitination in Mdm2 null cells. The extent of ubiquitination promoted by Pirh2 was similar to that promoted by Mdm2. Moreover, the level of p53 protein was lower when p53 was co-expressed with Pirh2 or with Mdm2. In the IP/Western blot shown in Figure 6D, immunoprecipitated p53 was heavily ubiquitinated in the presence of Pirh2 or Mdm2. These results provide evidence that Pirh2 functions independently of Mdm2. Next, we performed pulse-chase experiments to investigate the role of Pirh2 in regulating the stability of p53 protein. p53$^{-/-}$ Mdm2$^{-/-}$ double-null cells were transfected with a p53 expression vector in the presence or absence of Pirh2, pulse labeled with ^{35}S-methionine/cysteine and chased in non-radioactive medium. p53 protein was immunoprecipitated, separated by gel electrophoresis and visualized by autoradiography. Ectopically expressed p53 has a half-life of about 240 min in Mdm2 null MEFs. In the presence of Pirh2, the p53 half-life decreased to about 80 min (Figure 6E). These data indicate that Pirh2 regulates the stability of p53 in Mdm2 null cells.

To determine if Pirh2 has intrinsic ubiquitin-protein ligase activity, we used an in vitro ubiquitination assay (Lorick et al., 1999). Affinity purified GST-Pirh2 or GST alone were added to bacterial extracts containing recombinant E1 and E2 (UbcH5b), and His-tagged ubiquitin. Pirh2-mediated ubiquitination was readily detected and was dependent on the presence of E1 and E2 (Figure

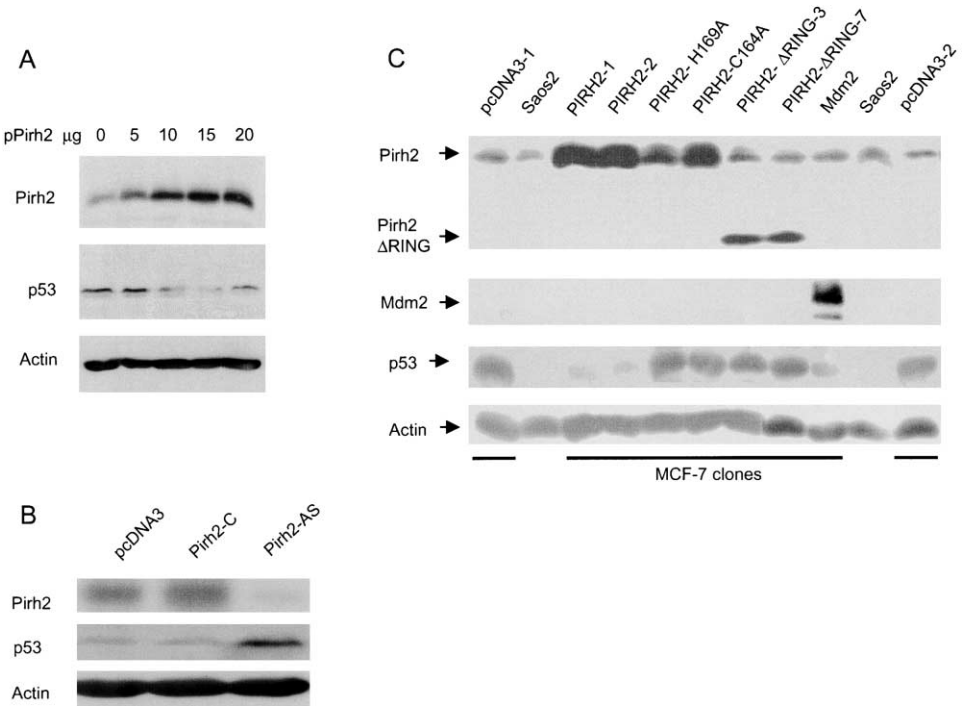

Figure 5. Pirh2 Interferes with the Steady-State Level of p53 Protein

(A) Wild-type p53 expressing MCF-7 cells were transfected with increasing amounts of the Pirh2 expression plasmid. The levels of ectopically expressed Pirh2 protein and endogenous p53 protein were determined by immunoblotting with Pirh2 antibodies or PAb1801, respectively. An antibody against β-actin was used as a loading control.

(B) BJT cells were exposed to *Pirh2* antisense oligonucleotide (AS) or to scrambled control oligonucleotide (C-oligo) for 48 hr. The levels of endogenous Pirh2 and p53 proteins were determined by immunoblotting with Pirh2 antibodies or PAb1801, respectively. An antibody against β-actin was used as a loading control.

(C) MCF-7 clones stably transfected with vectors expressing hPirh2 (PIRH2-1, PIRH2-2), Pirh2-H169A, Pirh2-C164A, Pirh2 ΔRING (PIRH2-ΔRING-3, PIRH2-ΔRING-7), Mdm2, or empty pcDNA3.1 vector (pcDNA3-1, pcDNA3-2) were subjected to immunoblotting using antibodies that recognize p53 (PAb1801), Mdm2, Pirh2, or β-actin. p53 null Saos2 cell extracts served as negative controls for p53 staining.

6F). To determine if p53 could serve as a substrate for Pirh2-dependent ubiquitination in vitro, reactions (lacking the bacterial extract) were supplemented with ^{35}S-labeled in vitro translated p53 (Figure 6G) or with purified GST-p53 fusion protein (Figure 6H). Ubiquitination of ^{35}S-labeled p53 was evaluated by SDS-PAGE and autoradiography and ubiquitination of purified GST-p53 was evaluated by Western blotting. Higher molecular weight species indicative of addition of ubiquitin moieties on p53 were seen only in the presence of added E1 and E2 (Figures 6G and 6H).

Pirh2 Interferes with the Transcriptional Activity of p53 Protein

To investigate the functional consequences of Pirh2 interaction with p53, we tested the effect of Pirh2 expression on p53-mediated transcriptional activation. Saos2 cells were cotransfected with a luciferase reporter construct (p21-Luc) containing the p53 binding site from the *p21^{WAF1}* promoter and p53, alone or in combination with Pirh2 or Mdm2. As shown in Figure 7A, Pirh2 and Mdm2 both repressed p53-mediated transactivation. Furthermore, a RING-less mutant of Pirh2 retained the ability to repress p53-mediated transactivation. Next, we transfected the p21-Luc reporter into MCF-7 clones that stably express Pirh2, Pirh2 ΔRING, or Mdm2. Luciferase activity was decreased in cells expressing Pirh2, Pirh2 ΔRING, and Mdm2 (Figure 7B). These data indicate that Pirh2 represses p53-dependent transactivation and that this repression does not require the RING domain of Pirh2. These data suggest that Pirh2 impairs the transactivation function of p53 without targeting it for degradation.

Pirh2 Interferes with the Growth Inhibitory Activity of p53

Next, we investigated the effect of Pirh2 on p53-dependent growth suppression. We used a cotransfection assay in which the pCMV-CD20 expression vector encoding the B cell surface marker CD20 was cotransfected with or without p53 into p53-negative H1299 cells. The number of CD20-positve cells was determined by flow cytometry 48 hr after transfection and a decrease in the number of CD20-positive cells provided a measure of p53-mediated cell death. Expression of p53 alone resulted in a reduction in cell viability and this was largely prevented by co-expressed Pirh2 (Figure 7C). To determine if this effect depended on Pirh2 E3 ligase activity, we studied three Pirh2 mutants: Pirh2 Δ120–137 is defective in binding p53, and Pirh2 ΔRING (deletion of residues 145–186) and Pirh2 1–137 are defective in p53 degradation and E3 ligase activity (Figure 5 and data

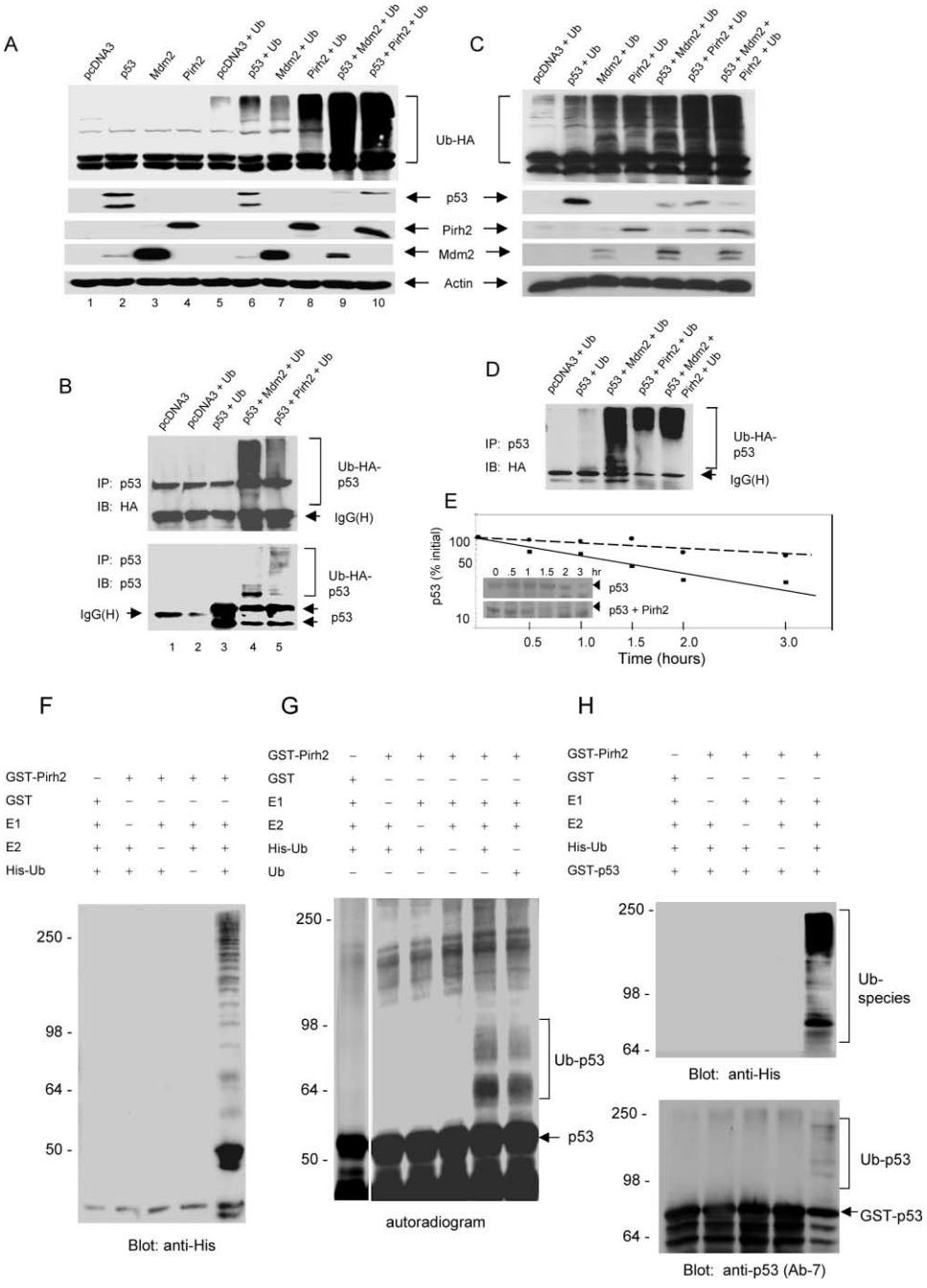

Figure 6. Pirh2 Promotes Ubiquitination and Serves as an E3 Ubiquitin Ligase

(A) Saos2 cells were transfected with vectors expressing HA-tagged ubiquitin (Ub), p53, Mdm2, and Pirh2 as indicated. Cell extracts were prepared 48 hr later, resolved by SDS-PAGE and analyzed by immunoblotting with the indicated antibodies.

(B) Similar to (A) except that equal amounts of cell extracts were immunoprecipitated with PAb1801 antibody against p53 and analyzed by immunoblotting with antibodies to HA (12CA5) (top) or p53 (Ab-7) (bottom).

(C) Similar to (A) except that $p53^{-/-}$ $Mdm2^{-/-}$ double-null MEFs were used as recipient cells for transfection using the indicated plasmids.

(D) Cell extracts were prepared following transfection of the $p53^{-/-}$ $Mdm2^{-/-}$ double-null MEFs with the indicated plasmids. Extracts were immunoprecipitated with FL-393 antibody against p53 and analyzed by immunoblotting with antibodies to HA.

(E) Pulse-chase analysis of ectopically expressed p53 in the presence or absence of Pirh2 in $p53^{-/-}$ $Mdm2^{-/-}$ double-null MEFs. Cells were metabolically labeled and chased for the indicated time points. p53 was immunoprecipitated with FL-393. The data shown in the inset were quantitated by phosphorimage analysis. The dashed line represents p53 alone, and the solid line represent p53 in the presence of Pirh2.

(F) GST-Pirh2 was evaluated for E3 activity in the presence of recombinant E1, UbcH5b (E2), and His-tagged Ub as indicated. Following the ubiquitination reaction, the samples were subjected to SDS-PAGE and immunoblotting with a His antibody to reveal ubiquitinated products.

(G) GST-Pirh2 was evaluated for its capacity to ubiquitinate ^{35}S-labeled p53 translated in a reticulocyte lysate. Each reaction contained ^{35}S-labeled p53 in addition to the indicated ubiquitination components. After the in vitro ubiquitination reaction, the samples were analyzed by SDS-PAGE and autoradiography.

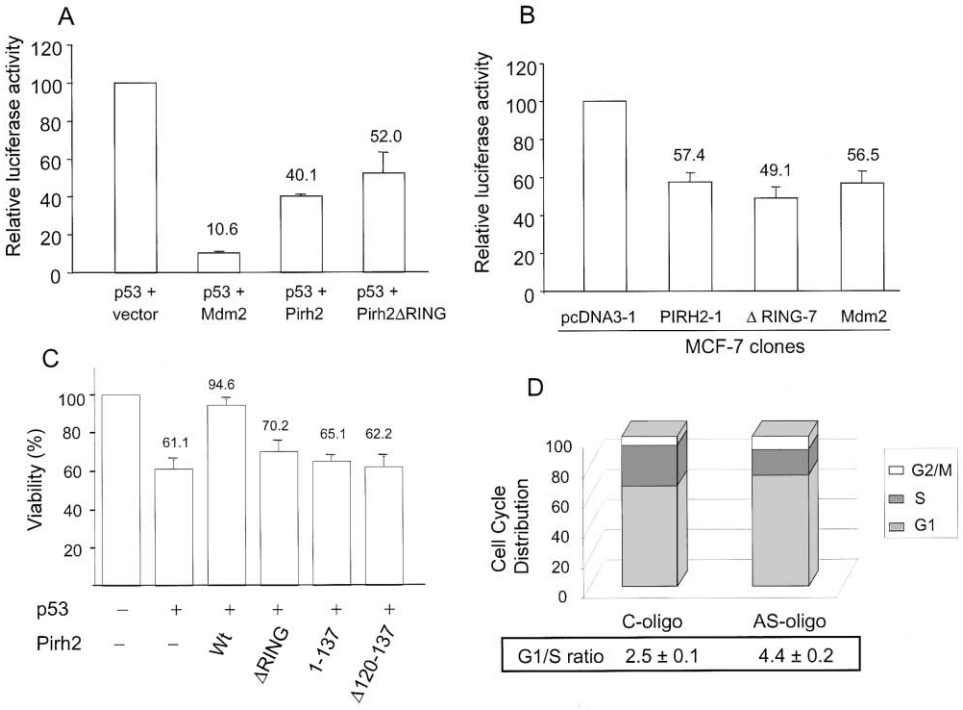

Figure 7. Pirh2 Interferes with the Transcriptional and Growth Suppressing Activities of p53

(A) Transcriptional activity of p53 protein was measured in Saos2 cells by cotransfection of a p21-Luc reporter plasmid and p53 together with Mdm2, Pirh2, Pirh2 ΔRING, or the empty expression vector pcDNA3.1 as control. Error bars indicate SEM (n = 3).

(B) MCF-7 clones stably expressing Pirh2 (PIRH2-1), Pirh2 ΔRING (ΔRING-7), Mdm2 (Mdm2), or pcDNA3.1 were transiently transfected with the p21-Luc reporter plasmid and luciferase activity was measured. Error bars indicate SEM (n = 4).

(C) The growth suppressing activity of p53 was measured in H1299 cells by cotransfection of a CD20 expression construct with pcDNA3-p53 (5 μg) and pcDNA3-Pirh2 (10 μg) or Pirh2 variants as indicated. The number of surviving CD20-positve cells was measured by flow cytometry 48 hr after transfection. Error bars indicate SEM (n = 3).

(D) BJT cells were exposed to hPirh2 antisense (AS) and control (C) oligonucleotides for 48 hr and subjected to cell cycle analysis by flow cytometry. The percentage of cells in G1, S, and G2/M was 67.3, 26.9, and 6.4 for the cells treated with control oligonucleotide, and 74.2, 17.0, and 8.8 for the cells treated with the antisense oligonucleotide. The results represent the average of triplicate experiments.

not shown). These mutants were unable to rescue cells from p53-mediated cell death (Figure 7C). These data suggest that the E3 ligase of activity of Pirh2 is required to block the growth suppressor function of p53.

Disruption of Pirh2 Potentiates p53-Dependent Cell Cycle Arrest

Given that overexpressed Pirh2 reduces the amount of endogenous p53 protein and that antisense-mediated disruption of Pirh2 increases the amount of endogenous p53 protein (Figure 5), we wished to determine if Pirh2 inhibition could potentiate the ability of endogenous p53 to arrest BJT fibroblasts in the G1 phase of the cell cycle. BJT cells were exposed to control or *Pirh2* antisense oligonucleotide and subjected to cell cycle analysis by propidium iodide staining and flow cytometry. Cells exposed to the control antisense oligonucleotide exhibited a normal cell cycle profile (Figure 7D) and unchanged levels of Pirh2 and p53 protein (Figure 5B). In contrast, BJT cells exposed to the *Pirh2* antisense oligonucleotide exhibited an increase in the proportion of cells in G1 and a decrease in the proportion of cells in S phase. This was reflected by an increase in the G1/S ratio from 2.5 to 4.4 and is consistent with arrest in the G1 phase of the cell cycle (Figure 7D). Antisense inhibition of Pirh2 expression resulted in elevated levels of p53 protein in BJT cells (Figure 5B). Taken together, these data demonstrate that Pirh2 is involved in the regulation of p53-mediated transcriptional activation, p53-mediated growth suppression, and p53-mediated checkpoint control.

Discussion

We propose that Pirh2 functions as a negative regulator of p53 and that it participates in an autoregulatory feedback loop with p53. In contrast with other p53 responsive genes, forced overexpression of Pirh2 in various recipient cells did not result in cell cycle arrest or in the induction of apoptosis. This study raises the possibility

(H) GST-Pirh2 was evaluated for its capacity to ubiquitinate purified His-p53. After the in vitro ubiquitination reaction, the samples were analyzed by SDS-PAGE and immunoblotting with a His antibody to reveal ubiquitinated products (top image) or with an antibody directed to p53 (Ab-7) to reveal ubiquitinated p53 species.

that Pirh2 overexpression in cancer cells may provide yet another mechanism to inactivate wild-type p53.

Our studies indicate that the RING-H2 domain of Pirh2 is necessary for degradation of p53 and to impair the growth suppressing activity of p53. In contrast, the RING-H2 domain of Pirh2 is not required for binding to p53 or to repress the transactivation function of p53. These data suggest that Pirh2-mediated degradation of p53 is required to inhibit its growth suppressing activity but not to inhibit its transactivation function. If this interpretation is correct, it implies that p53-mediated growth suppression involves transactivation-independent functions of p53.

An autoregulatory feedback loop involving p53 and Mdm2 is well established (Barak et al., 1993; Wu et al., 1993). Like *Mdm2*, the *Pirh2* gene is transcriptionally regulated by p53. In addition, both genes encode RING domain-containing proteins that are capable of physically interacting with p53 and inhibiting the transcriptional activity of p53. Moreover, Pirh2, like Mdm2, has ubiquitin-protein ligase activity and can target p53 for ubiquitination and degradation. In the present work, we have observed that Pirh2 functions independently of Mdm2. The striking level of functional similarity between Pirh2 and Mdm2 raises important questions about redundancy and the physiological significance of the multiple pathways that exert negative control over p53. In addition to Mdm2 and Pirh2, three other mechanisms have been reported to regulate p53 protein levels through ubiquitination: the HPV E6 protein targets p53 for ubiquitin-mediated degradation dependent on the cellular E6-AP ubiquitin ligase (Scheffner et al., 1993); the adenovirus E1B55K and E4orf6 proteins function together to promote p53 ubiquitination and degradation through a Cullin-containing E3 ubiquitin ligase complex (Querido et al., 2001); and JNK appears to target p53 for ubiquitin-mediated degradation through an Mdm2-independent mechanism (Adler et al., 1997; Fuchs et al., 1998). Negative control of p53 also occurs at the functional level though the action of Mdm4 (Shvarts et al., 1996; Jackson and Berberich, 2000), hSIRT1 (Vaziri et al., 2001; Luo et al., 2001) and the HDAC1 complex (Luo et al., 2000).

The complexity of the regulatory pathways that target p53 is illustrated by the fact that mice deficient for Mdm2 or Mdm4 die early in development. The embryonic lethality of *Mdm2*$^{-/-}$ and *Mdm4*$^{-/-}$ mice is completely rescued by loss of p53. Hence, Mdm4 and Mdm2 are unable to substitute for one another, and this suggests that the two proteins regulate p53 by nonoverlapping pathways (Parant et al., 2001). Pirh2, if present during the very early stages of mouse development, must also not be able to compensate for loss of Mdm2 or Mdm4. It will be informative to evaluate the expression patterns of *Pirh2*, *Mdm2*, and *Mdm4* in the developing embryo to determine if these genes are expressed in similar or different tissues. The possibility that p53 is targeted for ubiquitination by different pathways, depending on cell lineage or stage of differentiation, needs to be investigated. Furthermore, the fact that p53 assembles as a tetramer, that it can be covalently modified in response to various stress signals, and that it associates with various cellular and viral proteins, indicates that different forms of p53 co-exist within a cell. It is possible that these different forms of p53 are negatively regulated through distinct mechanisms.

Pirh2 binds to the central core domain of p53 (residues 82–292) and Mdm2 binds to the N-terminal 52 amino acid residues of the p53 protein (Chen et al., 1993). Whether or not both proteins can bind p53 simultaneously is not known. Recently, Gu et al. (2000) identified a region of p53 consisting of amino acids 92–112 that is required for Mdm2-mediated degradation, and they proposed the existence of a protein that functions with Mdm2 to target p53 for degradation. At least in vitro, Pirh2 and Mdm2 are each capable of promoting ubiquitination of p53. Moreover, ectopically expressed Pirh2 promotes ubiquitination in Mdm2 null cells. This does not exclude the possibility that the two proteins may function cooperatively under physiological conditions. Based on the observation that Mdm2-p53 complexes and JNK-p53 complexes are present in different phases of the cell cycle, Fuchs et al. (1998) suggested that Mdm2 and JNK regulate different functions of p53 during normal cell growth. It will be of interest to determine if the association between p53 and Pirh2 is cell cycle dependent, and whether the association and subcellular localization of these two proteins is influenced by cellular stress or DNA damage.

We have observed substantial heterogeneity in the induction of *Pirh2* transcripts following DNA damage in different cell lines. The p53-mediated transcriptional response to DNA damage is extremely complex. p53-regulated gene expression patterns differ not only in different cell types but also in response to different induction signals. There is heterogeneity in kinetics (timing, extent) of gene induction as well as on p53 dependency of gene induction. This heterogeneity is seen even in related cell lines derived from the same lineage (Yu et al., 1999; Zhao et al., 2000). The complexity of the p53 response may reflect the distinct pathways through which p53 can be activated in response to various stimuli (Appella and Anderson, 2001). It could also reflect differences in the affinity of various promoters for p53, such that some are responsive only to high levels of p53 or to certain modified forms of p53 (Resnick-Silverman et al., 1998). A transcription factor, like p53, will have many targets, and many of these will be codependent on other transcription and regulatory factors that may or may not be co-expressed with p53.

An important question raised by our results is whether Pirh2 targets other substrates in addition to p53. We believe this is likely for a number of reasons. First, ectopic Pirh2 expression in p53 null Saos2 cells resulted in ubiquitination of cellular substrates (Figure 5A). Second, Pirh2 is highly conserved with homologs in yeast, which do not have *p53*-like genes. *Drosophila* p53 protein is highly divergent from the mammalian p53 isotypes and may be more closely related to the p53 homolog, p63 (Yang et al., 2002). The presence of Pirh2 homologs in lower organisms raises the possibility that Pirh2 may also target the p53 homologs, p63 and p73. In preliminary experiments, we have observed binding between mammalian p73 and Pirh2 (data not shown). Third, endogenous *Pirh2* is expressed in *p53* null cells and so its dependency on p53 is not absolute. Lastly, individual E3s often control the ubiquitination of multiple substrates (Koepp et al., 1999) and so it is not unreasonable

to think that Pirh2 may target other proteins. Recently, a protein identical to Pirh2 was shown to bind to the human androgen receptor (Beitel et al., 2002).

Experimental Procedures

cDNA Cloning

RNAimage kits (GenHunter) were used for differential display according to manufacturer's protocol. Full-length cDNA was obtained by 5′-RACE PCR. Sequence analyses and alignments were carried out using the NCBI database and SeqWeb on the GCG Wisconsin Package Version 10.

Cell Culture and DNA Transfection

All cells were maintained in α-minimal essential medium supplemented with 10% fetal bovine serum. BJT cells were derived from normal human BJ fibroblasts that were immortalized by ectopic expression of the telomerase enzyme. BJT/DD cells express the C-terminal oligomerization domain of p53 (Vaziri et al., 2001). BaF3/DD cells were established by retroviral infection of BaF3 cells with a pBabe-p53DDneo. For the derivation of stable MCF-7 cell lines, cells were transfected using lipofectin and selected in 500 μg/ml of G418. For transient assays, plasmids or antisense oligonucleotides were transfected using calcium phosphate. Phosphorothioate-modified, HPLC-purified oligodeoxynucleotides were obtained from Invitrogen. hPirh2 AS: CCGGGCCGTCGCCGCCAT; scrambled control oligonucleotide: TGCCCTGCCGCGACGGCC. The hPirh2 AS oligonucleotide targets the translation initiation codon in human *Pirh2* mRNA.

Mammalian Expression Vectors

pcDNA3.1 served as the backbone mammalian expression vector for p53 and Pirh2. pCMV-Bam-Mdm2 (Oliner et al., 1993) was used for Mdm2 expression. The mammalian expression vector of His-Pirh2 was pTris-Ex-1 (Novagene). The RING domain of human Pirh2 was removed from pcDNA3.1-Pirh2 by PCR amplification of appropriate fragments and ligation. The Pirh2 mutants C164A and H169A were generated by site-directed mutagenesis (Quick Change, Stratagene).

Antibodies

p53 detection was carried out using PAb421 (Harlow et al., 1981), PAb1801 (Banks et al., 1986), FL-393 (Santa Cruz Biotechnology) or Ab-7 (Oncogene Research Products). Monoclonal antibodies against the HA-epitope (12CA5, Roche), the His-epitope (Novagen), and antibodies to β-actin (Sigma) and Mdm2 (Ab-1, Oncogene Research Products; smp14, Santa Cruz) were used for immunoprecipitation and immunoblotting. Antiserum against Pirh2 was raised in rabbits against the purified His-Pirh2 fusion protein and affinity-purified on GST-Pirh2 Sepharose beads or by adsorption to, and elution from, Pirh2 protein immobilized on nitrocellulose filters after SDS-PAGE.

Cell Viability Assay

H1299 cells were transfected using the calcium phosphate method with 3 μg CMV-CD20 in the presence or absence of pcDNA3-p53 (5 μg) and pcDNA3-hPirh2 or its variants (10 μg). Forty-eight hours after transfection, cells were stained with a FITC-conjugated anti-CD20 antibody (Pharmingen) in the presence of 1% BSA for 30 min at 4°C and the number of surviving CD20-positve cells was determined by flow cytometry. A decrease in the number of CD20-positive cells provided a measure of p53-mediated cell death.

Cell Cycle Analysis

BJT cells were washed once with PBS and incubated on ice in 0.1% sodium citrate, 0.2% NP-40, 200 μg/ml RNase A, and 50 μg/ml propidium iodide to release nuclei and stain the DNA. Cell cycle distribution was examined by flow cytometry using a FACScan flow cytometer (Becton Dickinson) and CellQuest software (Becton Dickinson). The relative proportion of cells in each phase of the cell cycle was determined using the automated ModFit program (Verity Software House Incorporated).

Northern Blot Analysis

Total RNA was isolated using the TRIzol reagent (Invitrogen) according to the manufacturer's instructions. Each RNA sample (10 μg) was run on a denaturing agarose gel and transferred to a positively charged nylon membrane. Hybridization of radioactive probes was done using standard conditions. The filters were exposed to X-ray film and the RNA was visualized by autoradiography. RNA levels were determined with a PhosphorImager using ImageQuant software (Molecular Dynamics).

Luciferase Assay

pGL3-E1bTATA contains a minimal promoter consisting of a TATA box downstream of one copy of the p53 binding site from the 5′ end of the $p21^{WAF}$ promoter and is referred to as p21-Luc (Resnick-Silverman et al., 1998). We replaced the $p21^{WAF1}$-derived sequence present in p21-Luc with the p53 binding sequence from mouse *Pirh2* or with an unrelated sequence of the same length to give rise to Pirh2-Luc and C-Luc, respectively. Expression vectors carrying either wild-type or mutant *p53* (5 μg) were cotransfected with the luciferase reporter construct (5 μg) into p53-negative Saos2 cells by calcium phosphate precipitation. A β-galactosidase reporter construct, pCMV-β-gal (Promega), was included in all the transfection mixes. Luciferase activity was measured 2 days posttransfection on samples containing equivalent amounts of protein using an LB9507 luminometer and the luciferase assay reagent (Promega); values were normalized to β-galactosidase activity.

Recombinant Protein Preparation

(See Supplemental Data available at http://www.cell.com/cgi/content/full/112/6/779/DC1).

GST Pull-down Assay

(See Supplemental Data available at above website.)

Metabolic Labeling and Immunoprecipitation Analysis

Saos2 cells were transfected with pcDNA3-Pirh2 alone or in combination with pcDNA3-p53. After 24 hr, the transfected cells were washed with methionine- and cysteine-free medium and starved for methionine and cysteine for 1 hr. Cells were metabolically labeled with 200 μCi of ^{35}S-methionine/cysteine for 2 hr. Subsequently, cells were collected by centrifugation, washed with PBS, lysed in 50 mM Tris-HCl [pH 8.0], 5 mM EDTA, 150 mM NaCl, and 0.5% NP-40, and immunoprecipitated with antibodies against Pirh2. The immune complexes were collected with protein A-agarose beads, washed four times with buffer containing 5% sucrose, 5.0 mM Tris-HCl [pH 7.4], 5 mM EDTA, 0.5 M NaCl, and 1% NP-40. The immunoprecipitates were analyzed by SDS-PAGE followed by autoradiography. For pulse-chase analysis, the $p53^{-/-}$ $Mdm2^{-/-}$ double-null cells were transfected with p53 and Pirh2 expression vectors and labeled 24 hr later with [^{35}S]methionine/cysteine as described above. The cells were washed and chased in non-radioactive medium for various periods of time. Lysates containing the same amount of trichloroacetic acid-insoluble radioactivity were immunoprecipitated with polyclonal antibodies to p53 (FL-393) and analyzed by gel electrophoresis and autoradiography.

Chromatin Immunoprecipitation

(See Supplemental Data available at above website.)

In Vitro Ubiquitination Assay

Ubiquitination assays were carried out by adding GST-Pirh2 (0.5–1 μg), rabbit E1 (40 ng, Calbiochem), UbcH5b (100 ng, Calbiochem), His-tagged ubiquitin (2 μg, Sigma) and 2 μl of BL-21 bacterial lysate in ubiquitination buffer (50 mM Tris-HCl [pH 7.4], 2 mM ATP, 5 mM MgCl, 2 mM DTT, 30 mM creatine phosphate, and 0.05 mg/ml creatine phosphokinase) to a final volume of 30 μl. The reactions were incubated at 30°C for 1.5–2 hr. The reactions were stopped with 2 × SDS loading buffer, heated to 95°C for 6 min, and the proteins were separated on a 10% SDS-PAGE. Ubiquitinated proteins were visualized by immunoblotting using a His antibody.

For p53 ubiquitination assays, ^{35}S-labeled p53 protein was synthesized by in vitro transcription and translation using the TNT T7 coupled reticulocyte lysate system (Promega). 2 × 10^4 cpm of in

vitro translated p53 were added to GST-Pirh2 (1–5 μg) and mixed on ice for at least 1 hr to form GST-Pirh2:p53 complexes. These complexes were then mixed with ubiquitination buffer and rabbit E1 (200 ng), UbcH5b (50 ng), and Ub (5 μg). The reactions were incubated at 30°C for 1.5–2 hr, stopped with 2 × SDS loading buffer, resolved on 10% SDS-PAGE and analyzed by autoradiography.

In Vivo Ubiquitination Assay

Saos2 cells were transfected with expression plasmids encoding p53, Pirh2, Mdm2, and HA-tagged ubiquitin either alone or in combination. Cells were collected 24 hr after transfection, lysed in modified RIPA buffer (2 mM Tris-HCl [pH 7.5], 5 mM EDTA, 150 mM NaCl, 1% NP-40, 1% deoxycholate, 0.025% SDS, and 1 mM PMSF), and analyzed by immunoblotting or by IP/immunoblotting. For immunoprecipitation, the lysates were sonicated and clarified by centrifugation at 4°C for 15 min to remove cellular debris. Lysates (1 mg) were incubated with antibody against p53 (PAb1801 or FL-393). The immunoprecipitates were collected with protein A-agarose beads, washed with RIPA buffer, separated on 10% SDS-PAGE, and transferred to PVDF membranes. The membranes were immunoblotted with polyclonal antibodies against p53 (Ab-7) or HA.

Acknowledgments

We thank C. Arrowsmith and A. Ayed for providing us with bacterial expression vectors encoding truncated p53 mutants; J. Manfredi for the p21-luciferase reporter construct; M. Oren for the p53DD plasmid; H. Vaziri for the BJT/DD cells; and M. Tyers for advice in setting up the in vitro ubiquitination assay. We thank our colleagues in the Benchimol laboratory for useful and critical discussions. This work was supported by the National Cancer Institute of Canada with funds from the Canadian Cancer Society and by the Canadian Institutes of Health Research. R.P.L. was supported initially by an Amgen Fellowship Award and is currently supported by a Fellowship Award from the Canadian Institutes of Health Research.

Received: March 8, 2002
Revised: February 14, 2003

References

Adler, V., Pincus, M.R., Minamoto, T., Fuchs, S., Bluth, M.J., Brandt-Rauf, P.W., Friedman, F.K., Robinson, R.C., Chen, J.M., Wang, X.W., et al. (1997). Conformation-dependent phosphorylation of p53. Proc. Natl. Acad. Sci. USA *94*, 1686–1691.

Appella, E., and Anderson, C.W. (2001). Post-translational modifications and activation of p53 by genotoxic stresses. Eur. J. Biochem. *268*, 2764–2772.

Banks, L., Matlashewski, G., and Crawford, L. (1986). Isolation of human-p53-specific monoclonal antibodies and their use in the studies of human p53 expression. Eur. J. Biochem. *159*, 529–534.

Barak, Y., Juven, T., Haffner, R., and Oren, M. (1993). Mdm2 expression is induced by wild type p53 activity. EMBO J. *12*, 461–468.

Beitel, L.K., Elhaji, Y.A., Lumbroso, R., Wing, S.S., Panet-Raymond, V., Gottlieb, B., Pinsky, L., and Trifiro, M.A. (2002). Cloning and characterization of an androgen receptor N-terminal-interacting protein with ubiquitin-protein ligase activity. J. Mol. Endocrinol. *29*, 41–60.

Borden, K.L.B. (2000). RING domains: master builders of molecular scaffolds? J. Mol. Biol. *295*, 1103–1112.

Chen, J., Marechal, V., and Levine, A.J. (1993). Mapping of the p53 and mdm-2 interaction domains. Mol. Cell. Biol. *13*, 4107–4114.

El-Deiry, W.S., Kern, S., Pietenpol, J.A., Kinzler, K.W., and Vogelstein, V. (1992). Definition of a consensus binding site for p53. Nat. Genet. *1*, 45–49.

Fang, S., Jensen, J.P., Ludwig, R.L., Vousden, K.H., and Weissman, A.M. (2000). Mdm2 is a RING finger-dependent ubiquitin protein ligase for itself and p53. J. Biol. Chem. *275*, 8945–8951.

Fuchs, S.Y., Adler, V., Buschmann, T., Yin, Z., Wu, X., Jones, S.N., and Ronai, Z. (1998). JNK targets p53 ubiquitination and degradation in nonstressed cells. Genes Dev. *12*, 2658–2663.

Gu, J., Chen, D., Rosenblum, J., Rubin, R.M., and Yuan, Z. (2000). Identification of a sequence element from p53 that signals for Mdm2-targeted degradation. Mol. Cell. Biol. *20*, 1243–1253.

Harlow, E., Crawford, L.V., Pim, D.C., and Williamson, N.M. (1981). Monoclonal antibodies specific for simian virus 40 tumor antigens. J. Virol. *39*, 861–869.

Haupt, Y., Maya, R., Kazaz, A., and Oren, M. (1997). Mdm2 promotes the rapid degradation of p53. Nature *387*, 296–299.

Honda, R., and Yasuda, H. (2000). Activity of MDM2, a ubiquitin ligase, toward p53 or itself is dependent on the RING finger domain of the ligase. Oncogene *19*, 1473–1476.

Honda, R., Tanaka, H., and Yasuda, Y. (1997). Oncoprotein MDM2 is a ubiquitin ligase E3 for tumor suppressor p53. FEBS Lett. *420*, 25–27.

Jackson, M.W., and Berberich, S.J. (2000). MdmX protects p53 from Mdm2-mediated degradation. Mol. Cell. Biol. *20*, 1001–1007.

Johnson, P., Chung, S., and Benchimol, S. (1993). Growth suppression of friend virus-transformed erythroleukemia cells by p53 protein is accompanied by hemoglobin production and is sensitive to erythropoietin. Mol. Cell. Biol. *13*, 1456–1463.

Jones, S.N., Roe, A.E., Donehower, L.A., and Bradley, A. (1995). Rescue of embryonic lethality in Mdm2-deficient mice by absence of p53. Nature *378*, 206–208.

Juven, T., Barak, Y., Zauberman, A., George, D.L., and Oren, M. (1993). Wild type p53 can mediate sequence-specific transactivation of an internal promoter within the mdm2 gene. Oncogene *8*, 3411–3416.

Koepp, D.M., Harper, J.W., and Elledge, S.J. (1999). How the cyclin became a cyclin: regulated proteolysis in the cell cycle. Cell *97*, 431–434.

Kubbutat, M.H.G., Jones, S.N., and Vousden, K.H. (1997). Regulation of p53 stability by Mdm2. Nature *387*, 299–303.

Levine, A.J. (1997). p53, the cellular gatekeeper for growth and division. Cell *88*, 323–331.

Lorick, K.L., Jensen, J.P., Fang, S., Ong, A.M., Hatakeyama, S., and Weissman, A.M. (1999). RING fingers mediate ubiquitin-conjugating enzyme (E2)-dependent ubiquitination. Proc. Natl. Acad. Sci. USA *96*, 11364–11369.

Luo, J., Su, F., Chen, D., Shiloh, A., and Gu, W. (2000). Deacetylation of p53 modulates its effect on cell growth and apoptosis. Nature *408*, 377–381.

Luo, J., Nikolaev, A.Y., Imai, S.I., Chen, D., Su, F., Shiloh, A., Guarente, L., and Gu, W. (2001). Negative control of p53 by Sir2α promotes cell survival under stress. Cell *107*, 137–148.

Momand, J., Zambetti, G.P., Olson, D.C., George, D., and Levine, A.J. (1992). The mdm-2 oncogene product forms a complex with the p53 protein and inhibits p53-mediated transactivation. Cell *69*, 1237–1245.

Montes de Oca Luna, R., Wagner, D.S., and Lozano, G. (1995). Rescue of early embryonic lethality in mdm2-deficient mice by deletion of p53. Nature *378*, 203–206.

Oliner, J.D., Pietenpol, J.A., Thiagalingam, S., Gyuris, J., Kinzler, K.W., and Vogelstein, B. (1993). Oncoprotein MDM2 conceals the activation domain of tumor suppressor p53. Nature *362*, 857–860.

Parant, J., Chavez-Reyes, A., Little, N.A., Yan, W., Reinke, V., Jochemsen, A.G., and Lozano, G. (2001). Rescue of embryonic lethality in Mdm4-null mice by loss of Trp53 suggests a nonoverlapping pathway with MDM2 to regulate p53. Nat. Genet. *29*, 92–95.

Prives, C., and Manley, J.L. (2001). Why is p53 acetylated? Cell *107*, 815–818.

Querido, E., Blanchette, P., Yan, Q., Kamura, T., Morrison, M., Boivin, D., Kaelin, W.G., Conaway, R.C., Conaway, J.W., and Branton, P.E. (2001). Degradation of p53 by adenovirus E4orf6 and E1B55K proteins occurs via a novel mechanism involving a Cullin-containing complex. Genes Dev. *15*, 3104–3117.

Resnick-Silverman, L., St. Clair, S., Maurer, M., Zhao, K., and Manfredi, J.J. (1998). Identification of a novel class of genomic DNA-binding sites suggests a mechanism for selectivity in target gene

activation by the tumor suppressor protein p53. Genes Dev. *12*, 2102–2107.

Scheffner, M., Huibregtse, J.M., Vierstra, R.D., and Howley, P.M. (1993). The HPV-16 E6 and E6-AP complex functions as a ubiquitin-protein ligase in the ubiquitination of p53. Cell *75*, 495–505.

Shaulian, E., Zauberman, A., Ginsberg, D., and Oren, M. (1992). Identification of a minimal transforming domain of p53: negative dominance through abrogation of sequence-specific DNA binding. Mol. Cell. Biol. *12*, 5581–5592.

Shvarts, A., Steegenga, W.T., Riteco, N., van Laar, T., Dekker, P., Bazuine, M., van Ham, R.C.A., van der Houven van Oordt, W., Hateboer, G., van der Eb, A.J., and Jochemsen, A.G. (1996). MDMX: a novel p53-binding protein with some functional properties of MDM2. EMBO J. *15*, 5349–5357.

Vaziri, H., Dessain, S.K., Ng-Eaton, E., Imai, S.I., Frye, R.A., Pandita, T.K., Guarente, L., and Weinberg, R.A. (2001). *hSIR2*^{SIRT1} functions as an NAD-dependent p53 deacetylase. Cell *107*, 149–159.

Vogelstein, B., Lane, D., and Levine, A.J. (2000). Surfing the p53 network. Nature *408*, 307–310.

Vousden, K.H. (2002). Activation of the p53 tumor suppressor protein. Biochim. Biophys. Acta *1602*, 47–59.

Wu, X., Bayle, J.H., Olson, D., and Levine, A.J. (1993). The p53-mdm-2 autoregulatory feedback loop. Genes Dev. *7*, 1126–1132.

Yang, A., Kaghad, M., Caput, D., and McKeon, F. (2002). On the shoulders of giants: p63, p73 and the rise of p53. Trends Genet. *18*, 90–95.

Yu, J., Zhang, L., Hwang, P.M., Rago, C., Kinzler, K.W., and Vogelstein, B. (1999). Identification and classification of p53-regulated genes. Proc. Natl. Acad. Sci. USA *96*, 14517–14522.

Zhao, R., Gish, K., Murphy, M., Yin, Y., Notterman, D., Hoffman, W.H., Tom, E., Mack, D.H., and Levine, A.J. (2000). Analysis of p53-regulated gene expression patterns using oligonucleotide arrays. Genes Dev. *14*, 981–993.

Accession Numbers

The Pirh2 sequence reported in this paper corresponds to AK018488.